Published in IET Signal Processing
Received on 13th March 2011
Revised on 26th February 2012
doi: 10.1049/iet-spr.2011.0093

ISSN 1751-9675

# Model-based estimation pursuit for sparse decomposition of ultrasonic echoes

*R. Demirli*[1] *J. Saniie*[2]

[1]*Center for Advanced Communications, Villanova University, Villanova, PA 19085, USA*
[2]*Department of Electrical and Computer Engineering, Illinois Institute of Technology, Chicago, IL 60616, USA*
*E-mail: ramazan.demirli@villanova.edu*

**Abstract:** Sparse signal decomposition techniques used for ultrasonic signal analysis are mainly based on the matching pursuit (MP) method using generic time-frequency dictionaries or more specific dictionaries designed for ultrasound measurements. These dictionary-based MP (DBMP) methods often perform inadequately in extracting meaningful echo components because of the rigid structure of pre-defined dictionaries. More recently emerged model-based signal decomposition methods decompose an ultrasonic signal in terms of parametric model echoes using successive echo partitioning, parameter estimation and echo subtraction. Although these techniques offer more flexibility in signal decomposition, they still use correlation in matching parametric model echoes to partitioned signal components. This study presents a model-based estimation pursuit (MBEP) method that utilises statistical estimation principles in echo matching, as a result provides a greater flexibility and control in signal decomposition. In particular MBEP algorithm utilises maximum a posteriori estimation and incorporates prior knowledge into signal decomposition. Unlike DBMP methods, MBEP obtains physically meaningful decompositions that have direct interpretations for ultrasonic testing. The superior performance of MBEP has been demonstrated using simulated and experimental ultrasonic signals.

## 1 Introduction

Sparse signal decomposition techniques based on the matching pursuit (MP) algorithm [1] have been extensively used for ultrasound signal processing because of their efficiency and ease of use in adaptive signal decomposition and feature extraction. These techniques aim to decompose an ultrasound signal in terms of a small number of functions chosen from a redundant dictionary. The decomposed functions are then used for subsequent analysis, for example, feature extraction and system identification.

The original MP algorithm decomposes a signal of length $N$ in terms of a small number functions (e.g. $M$, where $M = N$) chosen from the Gabor dictionary [1]. Researchers involved in acoustic signal processing have taken this generic signal decomposition approach a step further and utilised dictionaries specific to the ultrasound signals [2–4]. Lu and Michaels [2] presents a MP algorithm utilising a small size dictionary composed of a set of Gabor functions (GFs) tailored for a structural health monitoring system. Dictionary functions were designed according to spectral characteristics of the dominant (high-energy) echoes. Hong *et al.* [3] utilises a MP algorithm with a dictionary of chirp functions for non-destructive evaluation of guided-waves. The chirp dictionary was developed to represent echoes propagating through dispersive media. Cloutier [4] utilises a subset of the Gabor dictionary in designing a clutter rejection algorithm for Doppler ultrasound.

The dictionary-based MP (DBMP) techniques have several important shortcomings. Pre-defined dictionaries introduce errors in representing signal structures resulting from the rigid structure of the dictionary. It is often necessary to fine tune the matching functions using an optimisation algorithm. More importantly the MP method uses correlations (the inner products between signal residue and dictionary functions) to obtain best matching functions. Consequently, correlation often yields functions matched to global signal while smearing out local signal components. Third, the signal decomposition has to be performed within a fixed analysis window whose length is determined by the length of the largest scale dictionary function. The decomposition results obtained from fixed-size windows need to be combined to obtain the decomposition for the entire data. These shortcomings can be addressed using a more flexible signal matching strategy. The dictionary-free MP, first presented in papers [5, 6], is based on optimising the parameters of a normalised Gaussian function to match signal structures. This method has an inherent advantage over the DBMP. It is more versatile in selecting and optimising the elementary function to match relevant signal structures. This adaptive signal decomposition approach is also generic, that is, it can decompose any signal into normalised Gaussian functions [6]. However, the implementation of this technique involves parameter estimation which often requires designing a numerical optimisation algorithm specific for the model at hand. Despite its advantage this technique has been mostly overlooked in ultrasound signal analysis because of the challenges associated with its implementation.

Based on a dictionary-free MP approach, a model-based MP algorithm has been introduced in [7] for sparse signal decomposition of ultrasonic echoes. Inspired from the model-based ultrasonic signal analysis [8], this decomposition

technique is based on optimising the parameters of a generic echo to match local signal structures rather than using a pre-defined dictionary. Later, classical TF representations (TFRs) such as continuous wavelet transform (CWT), chirplet transform (CT), are embedded into this technique to partition echoes in TF domain and guide parameter estimation. CWT-based signal decomposition method has been used in ultrasonic data compression [9] and in pulse detection of amplitude scan (ASCAN) data [10]. More recently the Gaussian echo model in these techniques has been extended to Gaussian Chirplet (GC) model coupled with the CT-based partitioning. CT-based decomposition has been utilised in the analysis of dispersive ultrasonic echoes [11], and modelling reverberation echoes in multi-layered structures [12].

In this paper we generalise model-based MP methods by incorporating estimation-based matching strategies in signal decomposition. Incorporation of universal estimation techniques such as maximum likelihood estimation (MLE) and maximum a posteriori (MAP) estimation provides a greater flexibility and control in echo matching. In particular, we developed model-based estimation pursuit (MBEP) algorithm that utilises MAP parameter estimation. This algorithm matches the best model function to a partitioned data by estimating parameters under assumed prior knowledge [13]. Alternatively, a subset or all of the model parameters can be estimated using MLE. This degree of control in echo matching offers distinct advantages in ultrasonic signal analysis. One can decompose an ultrasonic signal into model echoes with certain desired characteristics and perform further analysis on model parameters.

In model-based decomposition algorithms [9, 11, 12], echo partitioning (i.e. windowing of data associated with a discrete echo) is a critical step before parameter estimation. Generally, a TFR of the ultrasonic signal is used to identify echo partitions in a hierarchy and apply a parameter estimation algorithm subject to the partitioned data [9, 11, 12]. Although TFRs have been shown to be effective in partitioning they are computationally involving and model dependent. In this paper we present an efficient echo partitioning algorithm based on signal envelope and instantaneous phase.

A sparse decomposition algorithm coupled with an echo partitioning based on the Gaussian echo model is presented in our earlier work [14]. In this paper, we generalise the Gaussian echo model [14] to the GC model, develop a MAP parameter estimation algorithm for the GC model and compare the algorithm performance to that of a dictionary-based MP algorithm for simulated and experimental ultrasonic data. Furthermore, we demonstrate that via incorporation of prior knowledge (e.g. echo bandwidth) in estimation, the MBEP can resolve closely spaced overlapping echoes that are otherwise not resolvable using DBMP techniques.

The rest of the paper is organised as follows. Next section presents the echo partitioning technique. Section 3 presents the MBEP algorithm using MAP and MLE methods. Section 4 presents sparse decomposition results using simulated and real ultrasonic data and compares the MBEP algorithm with a DBMP algorithm. Finally, Section 5 summarises the contributions and potential applications of the MBEP algorithm.

## 2 Ultrasonic echo partitioning via envelope and instantaneous phase

In sparse signal decomposition algorithms using DBMP, the decomposition is performed in a fixed length window. This approach requires partitioning the entire ultrasonic data into fixed length windows, performing function matchings and combining results from these windows. The size of the fixed length analysis window is often too large to focus on discrete echo components. Model-based signal decomposition methods [9, 11, 12] utilise partitioning based upon the time and frequency marginals of TFRs (e.g. CWT, CT). The decomposition algorithm adaptively partitions and decomposes the data into model echoes. However, the computational complexity of obtaining a TFR before signal decomposition and after each echo matching is significant. Furthermore, the TFR and parameter estimation are bounded tightly. A specific TFR is utilised based on the assumed echo model (e.g. GC) and model parameters are estimated based on the TFR of the partitioned echo. This section presents a new partitioning algorithm that is computationally efficient and independent of the echo model.

We exploit the bandpass property of ultrasonic echoes in echo partitioning. The analytic signal representation is useful for bandpass signal analysis. It allows simple determination of the envelope and instantaneous phase. The analytic signal for a real signal $s(t)$ is defined as

$$\psi(t) = s(t) + j\hat{s}(t) \tag{1}$$

where $\hat{s}(t)$ is the Hilbert transform (HT) of the signal. One can represent a discrete ultrasonic echo as

$$s(t) = \kappa(t)\cos\{2\pi f_c t + \varphi(t)\} \tag{2}$$

where $\kappa(t)$ is the envelope, $f_c$ is the centre frequency and $\varphi(t)$ is the instant phase of the signal. It is known that envelope and phase of the echo changes much slower than the sinusoidal term. Using this property, the analytic signal representation for the ultrasonic echo (2) is written as

$$\psi(t) = \kappa(t)\exp(j(2\pi f_c t + \phi(t))) \tag{3}$$

The magnitude of this signal is called envelope and identical to the magnitude of the real signal, that is

$$\kappa(t) = |\psi(t)| = \sqrt{s^2(t) + \hat{s}^2(t)} \tag{4}$$

Similarly, the phase of the real signal can be obtained from the phase of the analytic signal, that is

$$\varphi(t) = \angle\psi(t) = \tan^{-1}(\hat{s}(t)/s(t)) \tag{5}$$

The envelope detection based on HT is sensitive to noise even for high signal-to-noise ratio (SNR) levels. In order to obtain a smooth envelope we apply a frequency domain low-pass filtering (LPF) to the ultrasonic signal. The cut-off frequency of the LPF is set to the upper frequency limit of the measuring transducer. LPF provides a smooth envelope that is more robust for echo partitioning. The next step is to identify the most dominant echo component from the data using envelope and phase. To this end we determine the global maxima of the smooth envelope and place an analysis window of certain length centred at this peak point. Within the analysis window local maxima (peak point) and two neighbouring minima (end points) are sought. The local maxima mark the approximate peak point in time of the partitioned echo, whereas the two local minima neighbouring a local maxima mark the end points of the partition. The local minima and maxima are identified based upon the first and second derivatives of the smooth




doi: 10.1049/iet-spr.2011.0093

envelope. First derivative is used to find all local minima/maxima, and second derivative is used to separate local minima from maxima. The derivative operation is sensitive to noise, hence a smooth derivative operator is utilised to obtain first- and second-order derivatives. Some of the local minima and maxima are because of the small variations in the envelope and not necessarily mark the correct peaks and boundaries of echoes. Therefore the phase information is used to eliminate these spurious peaks and end points. More specifically phase-based constraints are enforced on the consecutive maxima/minima points based upon the time-domain characteristics of the transducer pulse. The phase difference between two consecutive local minima is required to be greater than a preset threshold value. Furthermore, the phase difference between two consecutive local maxima is required to be greater than a preset threshold value, and the phase difference between a consecutive minima followed by a maxima (and vice versa) is required to be greater than a preset threshold value. For example, the first and second thresholds can be chosen as $2\pi$ so that there is at least a full-cosine cycle between two consecutive local minima or maxima. The third threshold can be chosen as $\pi$ such that there is at least half a cosine cycle between a maxima and minima, and vice versa. These thresholds can be determined based on the time-domain characteristics of the transducer pulse used for the measurement.

We demonstrate this echo partitioning technique using a typical ultrasonic data. Fig. 1*a* displays the ultrasonic signal (solid line) obtained from a steel sample and its smooth envelope (dotted line). The peak points for the first three prominent echoes are shown in circles, whereas the corresponding border points are shown in diamonds. These points are obtained from the local minima and maxima of the envelope after enforcing phase-based constraints. Fig. 1*b* shows the unwrapped phase of the signal with these peak and border points marked. The phase differences between consecutive minima and maxima points are computed based on the unwrapped phase. The partition for the most prominent echo is determined by finding the global peak point of the envelope and the neighbouring two border points. This partitioned echo will be subject to model-based echo estimation. Then, the next prominent echo is windowed by identifying the largest peak and its neighbouring borders after removing the envelope of the first-matched echo from the global signal envelope. Using this technique in MBD, Fig. 1*c* displays the decomposed echoes (thick line) along with the measured signal (dotted line). The signal matching techniques using parameter estimation methods will be described in the next section.

## 3 Model-based estimation pursuit for sparse decomposition of ultrasonic echoes

In the conventional implementation of MP, functions are chosen from the dictionary of normalised functions (e.g. Gabor dictionary) to match signal residues [1]. The match criterion is based on the projection coefficient obtained by projecting the signal residue onto a dictionary function. MP first matches a function to the original signal. Then, this best matching function times the projection coefficient is subtracted from the signal to obtain the signal residue. At each iteration, a new dictionary function is matched to the current signal residue. When the energy of signal residue is a fraction of the energy of original signal the decomposition

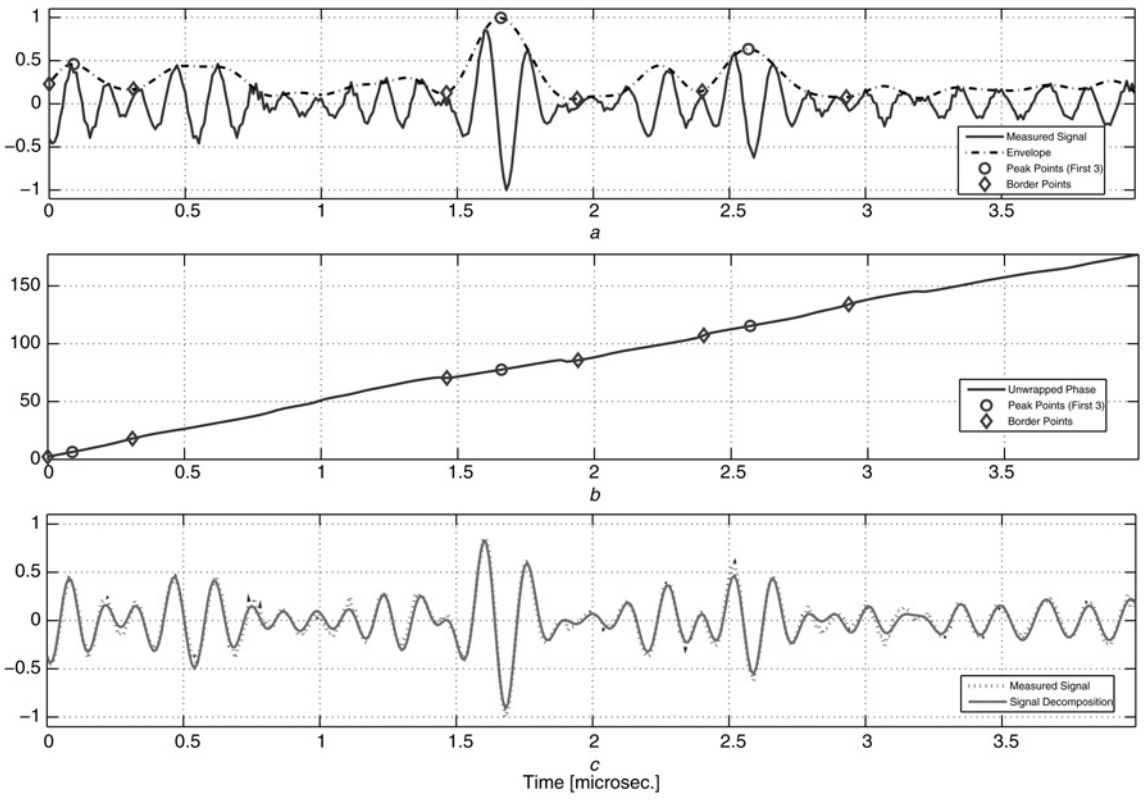


**Fig. 1** *Illustration of the ultrasonic echo partitioning technique using microstructure scattering echoes from a steel sample*

*a* Measured signal (solid line), smooth envelope (dotted line), peak points (disks) and border points (diamonds) identified for the first three prominent echoes
*b* Unwrapped phase (solid line) and its values at these peak and border points
*c* Measured signal (dotted line) and decomposition echoes (solid line)

is said to be complete. The final decomposition is a linear expansion of the best-matched dictionary functions. In the proposed MBEP method, a parametric echo model is optimised to best match discrete echo components obtained from the partitioning algorithm. Once the echo component is estimated it is subtracted from the data to obtain the next signal residue. Echo components are identified and estimated iteratively based on signal residues. The flowchart of MBEP is shown in Fig. 2. At the $n$th stage of the decomposition, the signal residue in an identified partition is represented by a model function and a remaining signal (i.e. next residue)

$$R^n y_{\mathrm{p}} = g(\theta) + R^{n+1} y_{\mathrm{p}} \tag{6}$$

where $R^n y_{\mathrm{p}}$ is the current signal residue, $R^{n+1} y_{\mathrm{p}}$ is the next signal residue and $g(\theta)$ is the model echo in the identified partition. The first signal residue is defined as the original signal, that is, $R^0 y = y$. In this paper, a real GC function is used for the echo model

$$g(\theta; t_k) = \beta e^{-\alpha(t_k-\tau)^2} \cos\{2\pi f_{\mathrm{c}}(t_k - \tau) + \psi(t_k - \tau)^2 + \varphi\},$$
$$k = 0, 1, 2, \ldots, K-1 \tag{7}$$

where $t_k = kT$ is the discrete time samples and $T$ is the sampling interval. The parameters of the GC function, bandwidth factor, arrival time, centre frequency, chirp rate, phase and amplitude, are stored in this order in a parameter vector $\boldsymbol{\theta} = [\alpha\ \tau\ f_{\mathrm{c}}\ \psi\ \varphi\ \beta]$. We assume that $R^{n+1} y_{\mathrm{p}}$ is white Gaussian noise (WGN). Although this assumption is not suitable for a long data trace containing a series of echoes, it is valid for an echo partition where the partition data can be considered as echo model corrupted with measurement noise. Further, we assume prior statistics (prior mean and covariance) for the parameter vector. Under these assumptions, the MAP estimation of the parameter vector can be obtained by solving

$$\theta_{\mathrm{MAP}} = \arg_\theta \min \|R^n y_{\mathrm{p}} - g(\theta)\|^2, \quad \text{while } E[\theta] = \mu_\theta \quad \text{and} \quad E[\theta\theta^{\mathrm{T}}] = C_\theta \tag{8}$$

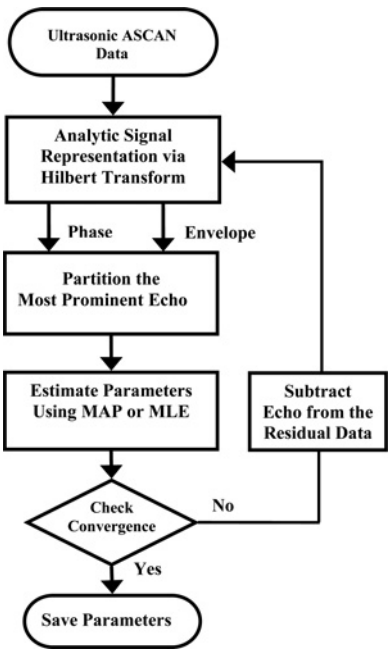


**Fig. 2** *Flowchart of the sparse signal decomposition algorithm*

Therefore parameter vector of the best matching function at stage $n$ is chosen by MAP estimation. If the prior statistics are ignored, the estimation problem in (8) states an MLE. In summary, MBEP algorithm using MAP estimation (MBEP–MAP) is outlined in the following computational steps:

1. Set iteration index $n = 0$ and first signal residue $R^0 y = y$.
2. Find the lower $i_{\mathrm{l}}$ and upper $i_{\mathrm{u}}$ indexes of the most prominent echo by means of envelope $\kappa$ and phase $\varphi$ of the current signal residue using the echo partitioning technique.
3. Partition the echo as $R^n y_{\mathrm{p}} = R^n y(i_l: i_{\mathrm{u}})$.
4. Find the best parameter vector by solving:

$$\theta_n = \arg_\theta \min \|R^n y_{\mathrm{p}} - g(\theta)\|^2 \quad \text{while } E[\theta] = \mu_\theta \quad \text{and} \quad E[\theta\theta^{\mathrm{T}}] = C_\theta$$

and compute the matching function: $g_n = g(\theta_n; t)$

5. Compute the next residue by removing the matching function

$$R^{n+1} y = R^n y - g_n$$

6. Update envelope and phase within the partition using analytic signal representation.
7. Check convergence: if $((\|R^{n+1} y\|^2)/||y||^2) \leq$ Threshold, STOP. Otherwise, set $n \rightarrow n+1$ and go to Step 2.

Step 1 of the algorithm initialises current signal residue as the original signal. Step 2 identifies the upper and lower indexes of the most prominent echo. Step 3 defines the partitioned echo from the current residue. Step 4 finds the best matching function for the current signal residue by optimising the parameters of the model echo, for example, GC function. Step 4, a MAP estimation problem, is essentially the most important step of the algorithm. An optimal solution is critical in achieving the best decomposition and requires a special care. In Appendix, we derived the MAP parameter estimation and provided a fast Gauss–Newton algorithm to efficiently solve this optimisation problem. The remaining steps of the algorithm are straightforward. Step 5 computes the next signal residue by subtracting the best matching GC function. Step 6 updates the envelope and phase within the partition window for the next partitioning operation. Step 7 checks for convergence: if the residue energy is some fraction of the original signal energy, the algorithm stops, otherwise a new model function is matched to current signal residue. The energy ratio in Step 7 is by definition an inverse SNR and can be set according to expected noise level.

The MBEP–MAP algorithm, through use of prior statistics, provides a control mechanism to focus on local signal structures. The DBMP algorithms generally match functions to global structures. This is in fact the major drawback of the MP algorithm [15, 16]. We demonstrate this phenomenon with a simulation example. Fig. 3*a* displays two partially overlapping GFs. GF is a special case of GC function when the chirp rate is zero. This example simulates two overlapping echoes in WGN (SNR is about 20 dB) sampled with 200 MHz sampling frequency. The parameter vectors used to generate these echoes are: $\theta_1 = [25\ (\mathrm{MHz})^2\ \ 0.8\ \mu\mathrm{s}\ \ 7.5\ \mathrm{MHz}\ \ 0\ \ 0\ \mathrm{rad}\ \ 1]$ and $\theta_2 = [23\ (\mathrm{MHz})^2\ \ 1.2\ \mu\mathrm{s}\ \ 7.0\ \mathrm{MHz}\ \ 0\ \ 0\ \mathrm{rad}\ \ 1]$ [see the parameter vector definition in (7)]. These two echoes are very close in centre frequency and bandwidths. When the




doi: 10.1049/iet-spr.2011.0093

DBMP algorithm is applied to this signal, a decomposition (Fig. 3*a*) consists of eight GFs (Fig. 3*b*) is obtained using the efficient implementation of the MP algorithm described in [17]. Note that only a subset of the Gabor dictionary (3 out of 9 scales, functions whose scales are closest to a 25 $(MHz)^2$ bandwidth-factor echo) is used so that more appropriate matches are obtained for the simulated echoes. The first GF matches partially both of the echoes, thus creates artificial signal components for successive matching. Some of the GFs (functions 4, 5 and 7 in Fig. 3*b*) are essentially generated to compensate for these artificial components. This decomposition, while it achieves a good representation of the signal as a whole (Fig. 3*a*), is not useful for echo separation.

One can improve the MP by concentrating on local signal structures and using better matching criteria. For example, the high resolution matching pursuit (HRMP) algorithm uses a local projection coefficient [15]. Through the use of b-spline functions, the matching signal is decomposed into sub-dictionary functions. HRMP chooses decompositions that maximise the lowest projection coefficient among those associated with the sub-dictionary functions. This results in decompositions locally adaptive to signal characteristics. Compared to MP, HRMP achieves a better temporal resolution. However, the frequency resolution of HRMP is not improved. When a matching function is decomposed into sub-dictionary functions, the assumptions are that sub-dictionary functions are symmetrical and contain the same frequency. More importantly, similar to MP, HRMP algorithm does not necessarily yield a meaningful decomposition for ultrasonic testing. On the other hand, MBEP provides a control mechanism to choose only certain characteristic waveforms that are deemed to be meaningful in the decomposition. In particular, for a generic ultrasonic measurement, one would expect echoes whose centre frequencies and bandwidths are within a range constituted by the transducer centre frequency and bandwidth. Therefore a meaningful decomposition should only contain waveforms whose centre frequencies and bandwidths are in this range. In fact, a blind decomposition (e.g. MP with Gabor dictionary) would return functions whose bandwidths may be either too narrow or too broad compared to the transducer bandwidth. Any waveform in the dictionary, although not necessarily meaningful for ultrasonic testing, will be included as long as it partially matches the signal.

The selection of prior statistics for model parameters is critical and application dependent. The rule of thumb is to adjust these prior parameters according to the desired functions in the decomposition. We demonstrate how to choose prior statistics and apply the MBEP–MAP algorithm for the simulated signal containing two overlapping echoes in Fig. 3. For this decomposition, the following prior mean is chosen for the parameter vector in this order, bandwidth factor, time-of-arrival, centre frequency, chirp rate, phase and amplitude: $E[\theta] = [25\ (MHz)^2\ t_0\ \mu s\ 6\ MHz\ 0\ 0\ rad\ a]$. The

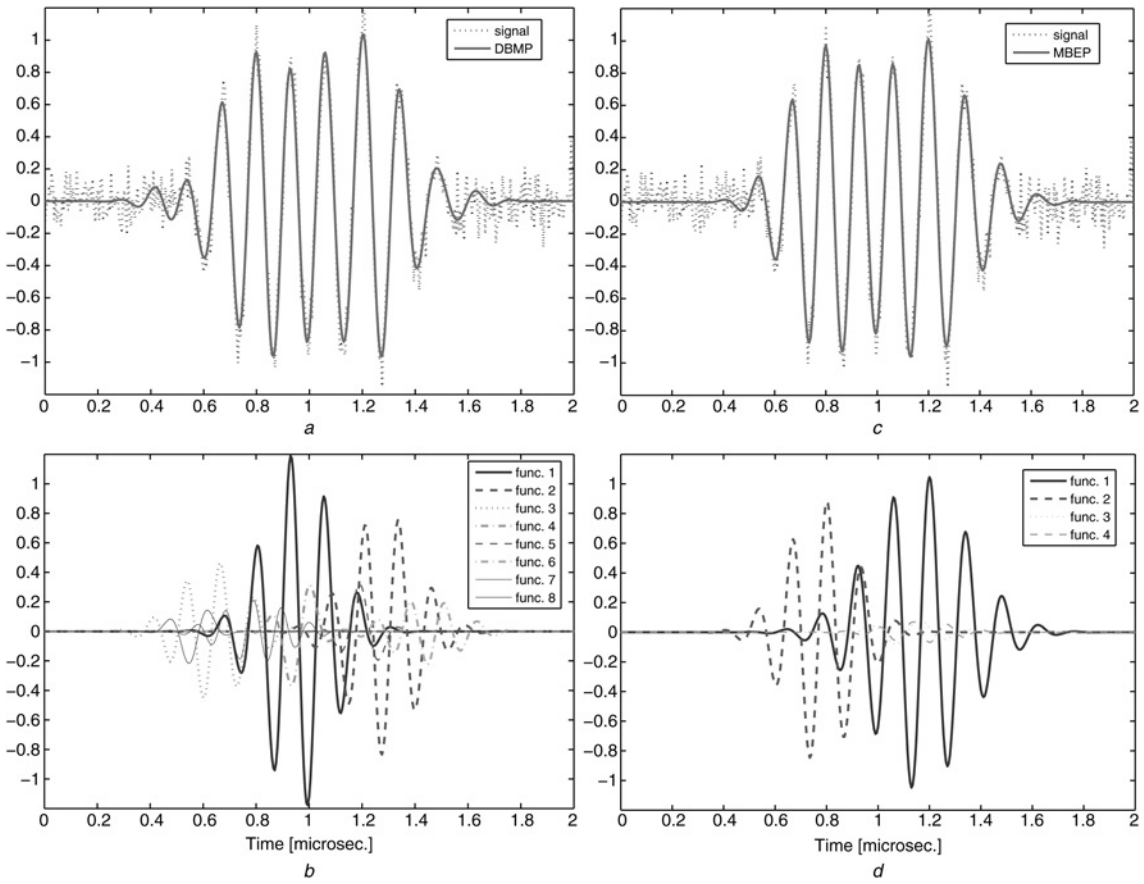


**Fig. 3** *Sparse decomposition of two overlapping echoes using DBMP and MBEP*

*a* Two overlapping echoes in noise (dotted line) and DBMP decomposition (solid line)
*b* Composing functions for *a*
*c* Two overlapping echoes as in *a* (dotted line) and MBEP decomposition (solid line)
*d* Composing functions for *c*
Residual energy is about the same as in *b*

prior means for arrival time ($t_0$) and amplitude ($a$) are obtained from the echo partitioning algorithm as the time point that produces a peak in the partitioned echo envelope and the peak value at this point, respectively. For bandwidth factor, centre frequency, chirp rate and phase, the prior means are chosen as constant according to our expectation. The first two parameters can be chosen based on the nominal centre frequency and bandwidth of the ultrasonic transducer. Assuming 0 for chirp rate and phase is a generic choice. To control variation from these values, a diagonal prior covariance matrix ($\boldsymbol{C}_\theta$) of size [6 × 6] is used where diagonal elements are the prior variances ordered same as in the prior mean vector above, that is, diag $\{C_\theta\} = \{100, 10, 2, 2, 1, 1\}$. Note that non-diagonal elements of $\boldsymbol{C}_\theta$ are set to zero so that there is no assumed prior correlation between any two parameter pairs. These prior statistics, when used in MBEP decomposition, will favour GC functions with centre frequencies varying around 6 MHz and bandwidth factors varying around 25 $(\text{MHz})^2$. These two constant parameters can be chosen based on the nominal centre frequency and bandwidth of the measuring transducer. Using these priors in the MAP–GN algorithm, the decomposition result is shown in Fig. 3*c* and composing GFs are shown in Fig. 3*d*. Unlike the DBMP decomposition (Fig. 3*b*), the composing functions clearly identify two distinct echoes with slightly different frequency content and produce a physically meaningful result. Furthermore, the decomposition required half the number of functions compared to that of the DBMP, thereby achieving a more compact representation of the signal.

For ultrasound measurements, a generic constraint can be set as follows. The magnitude spectrum of a matching function should be within the magnitude spectrum of the ultrasonic transducer. This can be done by setting the prior means of the bandwidth ($\alpha$) and centre frequency ($f_c$) parameters with respect to the nominal bandwidth and centre frequency of the transducer. The prior variances for these parameters can be set to desired values to allow certain amount of variations from the prior means. This approach favours model functions whose bandwidths are within the transducer bandwidth, hence offering a physically meaningful decomposition for ultrasonic measurements.

### 3.1 TF representation via MBEP

Although MBEP provides an explicit parametric representation of the signal, it is useful to visualise the decomposed signal in the TF domain. The MBEP algorithm, after $M$ iterations, decomposes a signal into $M$ -GC functions and a remaining residue

$$y = \sum_{n=0}^{M-1} g(\theta_n) + e \tag{9}$$

After the decomposition the great majority of signal energy is contained among the composing functions. Furthermore, at any stage of the decomposition a matching function is orthogonal to the signal residue [1]. These properties enable superimposing the TFR's of composing GC functions to obtain a TFR free of cross-terms [1]. Using the Wigner Ville distribution (WVD) formula of a real signal $x(t)$

$$\text{WVD}_x(t, \omega) = \frac{1}{2\pi}\int_{-\infty}^{\infty} x\left(t + \frac{\xi}{2}\right)x\left(t - \frac{\xi}{2}\right) \text{e}^{-j\omega\xi}\, \text{d}\xi \tag{10}$$

the TFR of a GC function (7) is obtained as

$$\text{TF}_g(t, f) = \frac{\beta^2}{2\pi\alpha}\, \text{e}^{-2\alpha(t-\tau)^2}\, \text{e}^{-(2/\alpha)[\pi(f-f_c)-\psi(t-\tau)]^2} \tag{11}$$

The above TFR is real and positive hence represents a joint time-frequency energy density function. Furthermore, it is expressed in terms of the parameters of GC function. As such, the TFR can be easily constructed if the parameters of GC are known. The TFR of signal $\boldsymbol{y}$ expressed in terms of GC functions (10) is a superposition of the TFR of each composing GC function

$$\text{MPTF}\{y\} = \sum_{m=0}^{M-1} \text{TF}\{g(\theta_m)\} \tag{12}$$

For a reference, the short time Fourier transform (STFT) of a signal $x(t)$, windowed by a function $h(t)$of duration $\Delta$ is defined as

$$\text{STFT}_x(t, \omega) = \int_{t-\Delta/2}^{t+\Delta/2} x(\tau)h(\tau - t)\, \text{e}^{-j\omega\tau}\, \text{d}\tau \tag{13}$$

The spectrogram (SP) is defined as the energy distribution of STFT and will be used as a reference TFR in comparison to MPTF

$$\text{SP}_x(t, \omega) = |\text{STFT}_x(t, \omega)|^2 \tag{14}$$

## 4 Sparse decomposition of simulated and experimental ultrasonic data

### 4.1 Simulated ultrasonic data

We test the proposed MBEP algorithm on simulated ultrasonic data and compare its performance to the DBMP algorithm. A simulated ultrasonic signal consists of GFs corrupted with WGN (SNR is about 10 dB) is shown in Fig. 4*a*. These functions simulate a number of overlapping echoes measured with a hypothetical ultrasonic transducer that has a certain centre frequency and bandwidth. MBEP–MAP and DBMP algorithms are applied to this signal. For MBEP–MAP algorithm, the prior mean and variance for bandwidth factor parameter are set to 25 and 100 $(\text{MHz})^2$, and the prior mean and variance for centre frequency are set to 5 and 10 (MHz, respectively. (These prior mean and variance parameters define a normal distribution.) These values are chosen so that the bandwidth factor will change in range [15 35] $(\text{MHz})^2$ and centre frequency will change in range [2 8] MHz, both in a 67% probability (i.e. the range is plus/minus one standard deviation from the prior mean). It is assumed that the simulating transducer generates echoes with centre frequencies and bandwidth factors in these ranges. In real ultrasonic measurements these values should be chosen in accordance with spectral characteristics (i.e. nominal bandwidth and centre frequency) of the measuring transducer. The other parameters (arrival time, phase and amplitude) are estimated freely (i.e. without any prior knowledge) by imposing very large prior variances. Note that MAP estimation can be switched to MLE by assuming very large prior variances on a subset or all of the parameters [13]. Under these assumptions, the MBEP–MAP decomposition is shown in Fig. 4*a* with a solid line and the DBMP decomposition is shown in a dashed line. Comparing the decomposed signals




doi: 10.1049/iet-spr.2011.0093

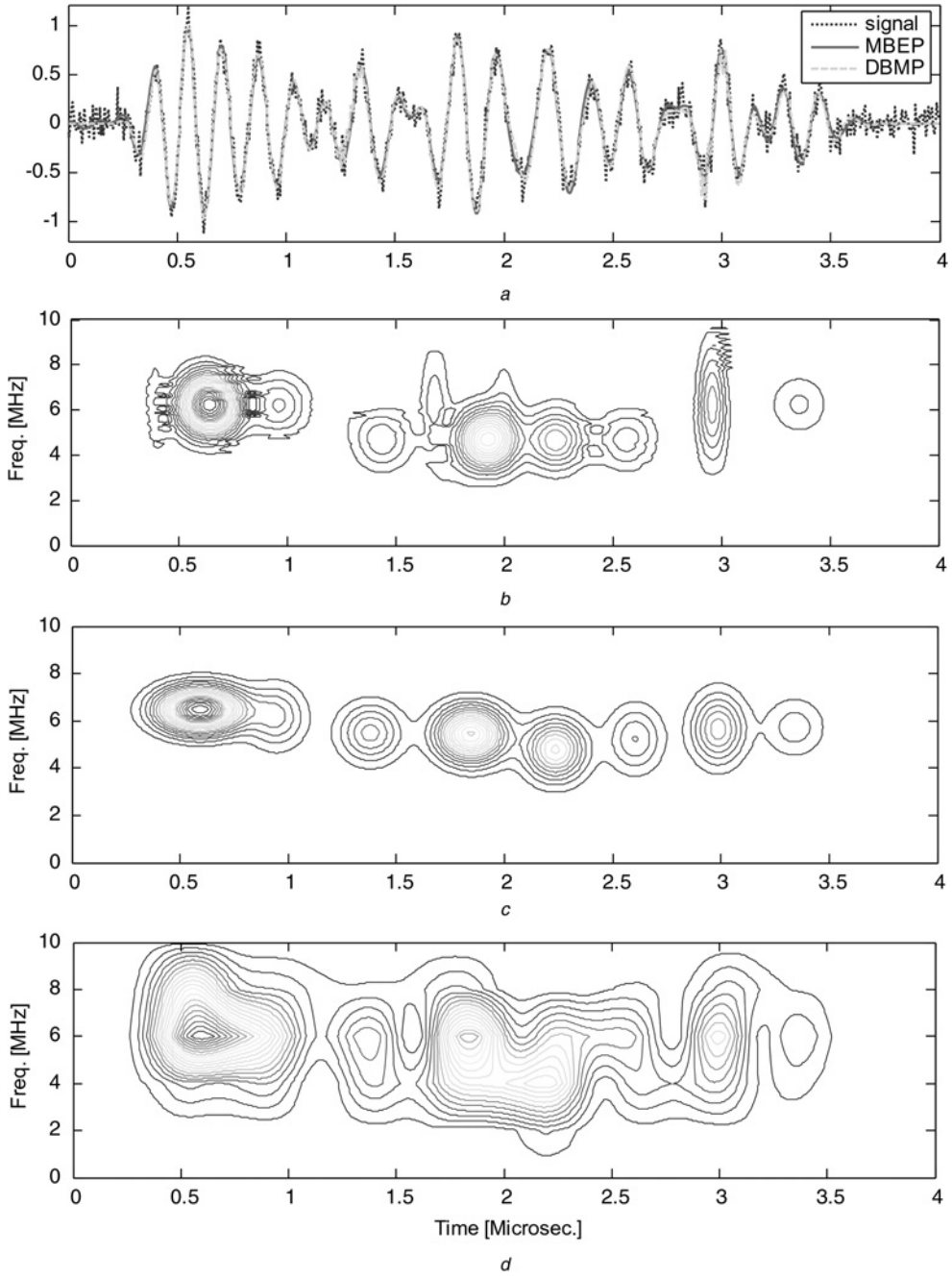


**Fig. 4** *Sparse decomposition of simulated ultrasonic echoes*

*a* Simulated echoes (dotted line), MBEP–MAP decomposition (solid line) utilising 15 GFs and DBMP (dashed line) decomposition utilising 28 GFs at about the same residual energy level
*b* TF distribution via DBMP
*c* TF distribution via MBEP–MAP
*d* TF distribution via SP

(Fig. 4*a*), it is difficult to make a distinction between these two decompositions. However, at about the same residual noise energy level, MBEP–MAP decomposition contains 15 GFs while DBMP decomposition contains 28. The estimated parameters using MBEP and DBMP are listed in Tables 1(*a*) and (*b*), respectively. The inspection of bandwidth and centre frequency parameters reveals the disparity in these two sets of composing GFs. Note that these two parameters are primarily responsible for the shape of the GF. DBMP decomposition contains GFs with two scales (32 and 64) which are closest to the simulating transducer's nominal bandwidth. Note that the scale parameter is directly proportional to the bandwidth of the GF. On the other hand, MBEP–MAP generates functions whose bandwidths and centre frequencies exhibit much less variation because the prior variances constrained these parameters (see Table 1*a*). Enforcing a constraint on these parameters allow waveforms whose bandwidths and centre frequencies are close to the transducer bandwidth, hence forcing the MBEP algorithm to extract discrete echo components.

The differences between these two approaches can be appreciated better when these GFs are mapped to the TF plane to obtain TFRs. The MBEP–TF and DBMP–TF are displayed in Figs. 4*b* and *c*, respectively. For comparison with a model-free time-frequency representation, the

**Table 1** Estimated parameters of GFs using

(a) MBEP

| Function number | Bandwidth factor, $MHz^2$ | Arrival time, μs | Centre frequency, MHz | Amplitude |
|---|---|---|---|---|
| 1 | 15.3703 | 0.5915 | 6.4777 | 1.0124 |
| 2 | 23.2431 | 1.8440 | 5.4341 | 0.9253 |
| 3 | 28.7231 | 2.2352 | 4.7839 | 0.7910 |
| 4 | 37.4969 | 2.9870 | 5.6467 | 0.7146 |
| 5 | 26.7318 | 1.3800 | 5.4875 | 0.5974 |
| 6 | 31.4702 | 0.9467 | 6.1795 | 0.5508 |
| 7 | 35.0307 | 2.6036 | 5.2325 | 0.5512 |
| 8 | 28.1641 | 3.3398 | 5.7256 | 0.4204 |
| 9 | 29.1470 | 0.6556 | 6.5411 | 0.1138 |
| 10 | 27.1325 | 1.9054 | 4.5940 | 0.0995 |
| 11 | 28.7363 | 1.7495 | 5.8665 | 0.1103 |
| 12 | 25.0558 | 0.5400 | 6.4890 | 0.0978 |
| 13 | 25.2501 | 0.1929 | 5.9010 | 0.0906 |
| 14 | 30.4418 | 2.9971 | 7.4707 | 0.0837 |
| 15 | 27.8713 | 0.6511 | 7.2670 | 0.0708 |

(b) DBMP

| Function number | Scale | Arrival time, μs | Centre frequency, MHz | Projection coefficient |
|---|---|---|---|---|
| 1 | 64 | 0.64 | 6.0868 | −5.5777 |
| 2 | 64 | 1.92 | 0.1473 | −4.4931 |
| 3 | 64 | 2.24 | 6.1359 | −3.1948 |
| 4 | 32 | 2.96 | 6.0868 | −2.9042 |
| 5 | 64 | 0.96 | 6.0868 | −2.5075 |
| 6 | 64 | 1.44 | 6.1359 | −2.4240 |
| 7 | 64 | 2.56 | 6.1359 | 2.3026 |
| 8 | 32 | 1.68 | 0.1963 | 1.9847 |
| 9 | 64 | 3.36 | 0.1963 | −1.8225 |
| 10 | 32 | 0.40 | 0.1963 | −1.5799 |
| 11 | 32 | 2.00 | 0.1963 | 1.4681 |
| 12 | 32 | 0.72 | 6.0868 | 1.1963 |
| 13 | 32 | 3.04 | 0.2945 | −1.0566 |
| 14 | 64 | 1.76 | 0.0982 | −0.9674 |
| 15 | 64 | 1.28 | 0.1963 | −0.9337 |
| 16 | 32 | 3.12 | 6.1850 | 0.8509 |
| 17 | 32 | 2.40 | 6.0868 | 0.8463 |
| 18 | 32 | 2.64 | 0.1963 | 0.6375 |
| 19 | 64 | 1.76 | 5.9887 | 0.6078 |
| 20 | 64 | 0.96 | 0.1473 | 0.5628 |
| 21 | 64 | 0.48 | 0.0491 | 0.5291 |
| 22 | 32 | 1.52 | 6.0868 | 0.5167 |
| 23 | 32 | 2.88 | 0.1963 | −0.4731 |
| 24 | 64 | 0.64 | 5.9887 | 0.4572 |
| 25 | 32 | 2.24 | 6.0868 | 0.4517 |
| 26 | 32 | 2.96 | 4.7124 | 0.4274 |
| 27 | 32 | 1.28 | 4.5160 | 0.4063 |
| 28 | 32 | 2.96 | 1.2763 | −0.3821 |

spectogram (SP) is displayed in Fig. 4*d*. All TFR plots are in linear scales. The SP is implemented based on (13) and (14) using a Hanning window of length equal to the duration of transducer impulse response. Although SP smears the true TF, it is used here as a reference to other TFRs. Both MBEP–TF and DBMP–TF approximately trail the SP, that is, they do not create artificial TF components such as cross-terms. Further, compared to the DBMP–TF, MBEP–TF provides a more concentrated and smooth energy distribution.

It is important to point out that the primary aim of MBEP decomposition is to obtain physically meaningful echo structures from the ultrasonic data so that the parameters of these echoes (e.g. time-of-arrival, centre frequency, bandwidth, amplitude etc.) can be correlated with the physical properties of reflectors. On the other hand, conventional MP techniques seek the sparsest decomposition which contains echo structures not necessarily meaningful for ultrasonic testing.

### 4.2 Noise analysis

We analyse the performance of MBEP decomposition with varying noise level. As discussed in Section 4.1, we




doi: 10.1049/iet-spr.2011.0093

simulated ultrasonic data consists of a number of overlapping GFs measured with a hypothetical ultrasonic transducer that has a certain centre frequency and bandwidth. As before, the prior mean and variance for bandwidth factor parameter are set to 25 and 100 $(\text{MHz})^2$, and the prior mean and variance for centre frequency are set to 5 and 10 MHz, respectively. The decomposition is observed by adding increased variance of zero-mean WGN to the simulated echoes. The decomposition results for different noise levels are shown in TF domain for easier comparison. The TFR of the noise-free echoes obtained via MBEP is shown in Fig. 5*b*, whereas the TFRs of noisy echoes are shown in Figs. 5*c* for 20 dB, *d* for 10 dB, *e* for 5 dB and *f* for 2.5 dB, respectively. For comparison purpose, the number of reconstructed echoes is fixed to 15. As it is seen from the TFR plots, eight dominant echoes are always identified albeit the noise level is increased. However, a small degree of variations exists between the decompositions down to the 10 dB SNR (see Figs. 5*b*–*d*). This variation is partially owing to the fact that parameter estimation of the partitioned echo varies with noise. This variation is also because of greedy nature of the decomposition, that is, dominant echoes are always extracted first, as a result, the variation in the preceding steps of the decomposition carries over to the subsequent steps. The variation due to parameter estimation has been thoroughly analysed in our previous works via Cramer-Rao lower bounds (CRLBs) for Gaussian echo [8] and GC models [11]. It has been shown that parameter estimation is unbiased and minimum variance (i.e. CRLBs are attained) for SNR levels as low as 5 dB for GF and 10 dB for GC [8, 11]. It is clear that above a certain noise level parameter estimation will be inefficient, so will be the MBEP decomposition based on parameter estimation. It can be clearly stated that the MBEP decomposition in high SNR regimes (10 dB and above) will be efficient and the variation owing to noise will be small.

### 4.3 Real ultrasonic data

MBEP signal decomposition algorithm has been tested and compared with DBMP decomposition on real ultrasonic data (see Fig. 6*a*) acquired from a large-grained steel block that contains a drilled flaw. The data are acquired using a broadband transducer with 5 MHz centre frequency. The sampling rate is 200 MHz. The signal contains grain scattering echoes and a backscattered echo from the flaw. First, we obtain DBMP decomposition on this data using a subset of Gabor dictionary with closest scales to the transducer bandwidth as in the simulated data. The decomposed signal containing 52 dictionary functions are plotted along with the measured data in Fig. 6*a*. The corresponding TFR is also displayed in Fig. 6*b*. The TFR is useful for visualisation and inspection of the energy distribution of composing echoes. For MBEP decomposition of this experimental data, we obtain prior statistics for the bandwidth factor ($\alpha$) and centre frequency ($f_c$) parameters according to the following procedure. The transducer impulse response is obtained by making an echo measurement from a planar surface reflector in water [8]. We then estimate the parameters (centre frequency and bandwidth) of the transducer impulse response by fitting a GC model to the measured echo. The estimated bandwidth factor, 30 $(\text{MHz})^2$, and centre frequency, 6.2 (MHz), are used as prior means. The bandwidth and centre frequency parameters of decomposed echoes are expected to vary around these values. The prior variances for these parameters are set to 100 $(\text{MHz})^2$ and 10 MHz, respectively, to control variation from the prior means. These priors will constrain a range of [20 40] $(\text{MHz})^2$ for bandwidth factor and a range of [3.2 9.2] MHz for centre frequency. Using these parameters, the decomposition signal containing 52 model echoes is displayed in Fig. 6*c* (solid line) along with the measured signal (dotted line). Furthermore, the TFR of the decomposed echoes using MBEP–TFR formula in (12) is shown in Fig. 6*d*. Although the decomposed signals in time domain (see Figs. 6*a* and *c*) seem almost identical and yield almost the same residual energy, the TFRs reveal the difference between the MBEP and DBMP decompositions. First, MBEP algorithm obtains a smoother and more concentrated TFR of the data as it can be observed from Figs. 6*b* and *d*. Most importantly, MBEP algorithm extracts physically meaningful echoes such as those obtained from point or geometric reflectors. As such, these echoes are useful for system identification under ultrasonic testing. On the other hand, DBMP decomposition creates artificial echo components (see, e.g. TF contours between 2 and 3 μs, 10.5 and 11.5 μs and about 14 μs in Fig. 6*b*). These echoes are the byproducts of the DBMP hence do not provide useful information for ultrasonic testing.

The ultrasonic signal decomposition (such as that in Fig. 6*c*) obtained by MBEP algorithm possesses not only the known benefits of a sparse representation such as compression and denoising advantage but also physical interpretation of the received signal in terms of ultrasonic testing. The parameters of the composing echoes can be linked to the location, size and orientation of reflectors and attenuation characteristics of the propagation path [8]. As a result these parameters can be used for ultrasonic testing such as feature extraction and classification. For example, ultrasonic flaw detection in presence of microstructure scattering is challenging because flaw echoes are masked by scattering echoes. It is known that flaw echoes exhibit high energy profiles at low frequencies whereas grain echoes exhibit low energy profiles at high frequencies. This property can be exploited using MBEP decomposition results for flaw detection. The high energy density circles at low frequency levels in the TF plot (Fig. 6*d*) represent the flaw echo. One can determine the exact location, frequency and energy of this echo by examining the parameters of the associated GC function. Another desirable property of this decomposition is its ability to extract echoes in a hierarchical order from high to low energy echoes. This is illustrated in Fig. 7 where the residual energy decreases monotonically after each echo estimation and removal.

Finally, the overall computational demand of the MBEP algorithm is practical. For example, the experimental data presented in Fig. 6*a* containing 2048 samples ($N = 2048$) takes 52 matching functions for decomposition, and each matching function takes about 20 MAP–GN iterations. On a dual-core Pentium PC processor with 1.66 GHz clock-rate, the MATLAB implementation of the algorithm takes about 1.1 s to process this data including the pre-processing (envelope detection and filtering) operations. The MAP–GN algorithm presented in Appendix is rather fast. The major computational load for one MAP–GN iteration is six inner products (see (19), Appendix) in a reduced dimension $L$ and the average partitioned echo length (e.g. $L < 100$).

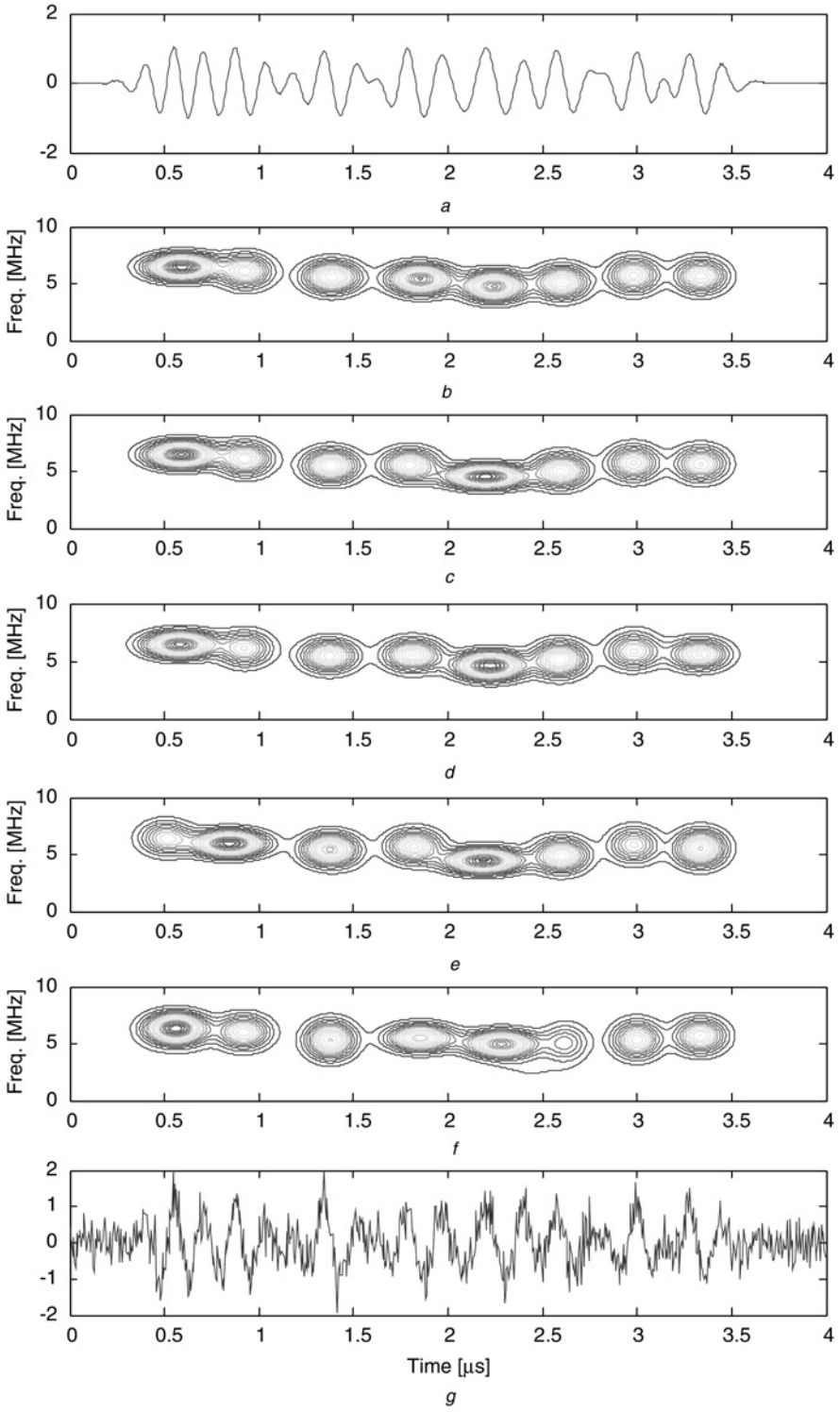


**Fig. 5** *MBEP decomposition of ultrasonic echoes with varying level of noise*

*a* Simulated echoes (noise free)
*b* TFR (contour plot) for *a*
*c* TFR for SNR 20 dB
*d* TFR for SNR 10 dB
*e* TFR for SNR 5 dB
*f* TFR for SNR 2.5 dB
*g* Simulated echoes corresponding to the TFR in *f*

Since $L$ is much shorter than the data length $N$, on average, one GC echo matching requires $120xL$ inner products. This is significantly smaller than the number of inner products ($N \log_2 N = 22528$) the DBMP algorithm [1] would take for one MP iteration. Note that this computation time (1.1 s) can be reduced further with an efficient implementation of the algorithm. Overall, this low computational complexity offers a very practical and efficient solution for real-time ultrasonic signal decomposition.



*IET Signal Process.*, 2012, Vol. 6, Iss. 4, pp. 313–325
doi: 10.1049/iet-spr.2011.0093

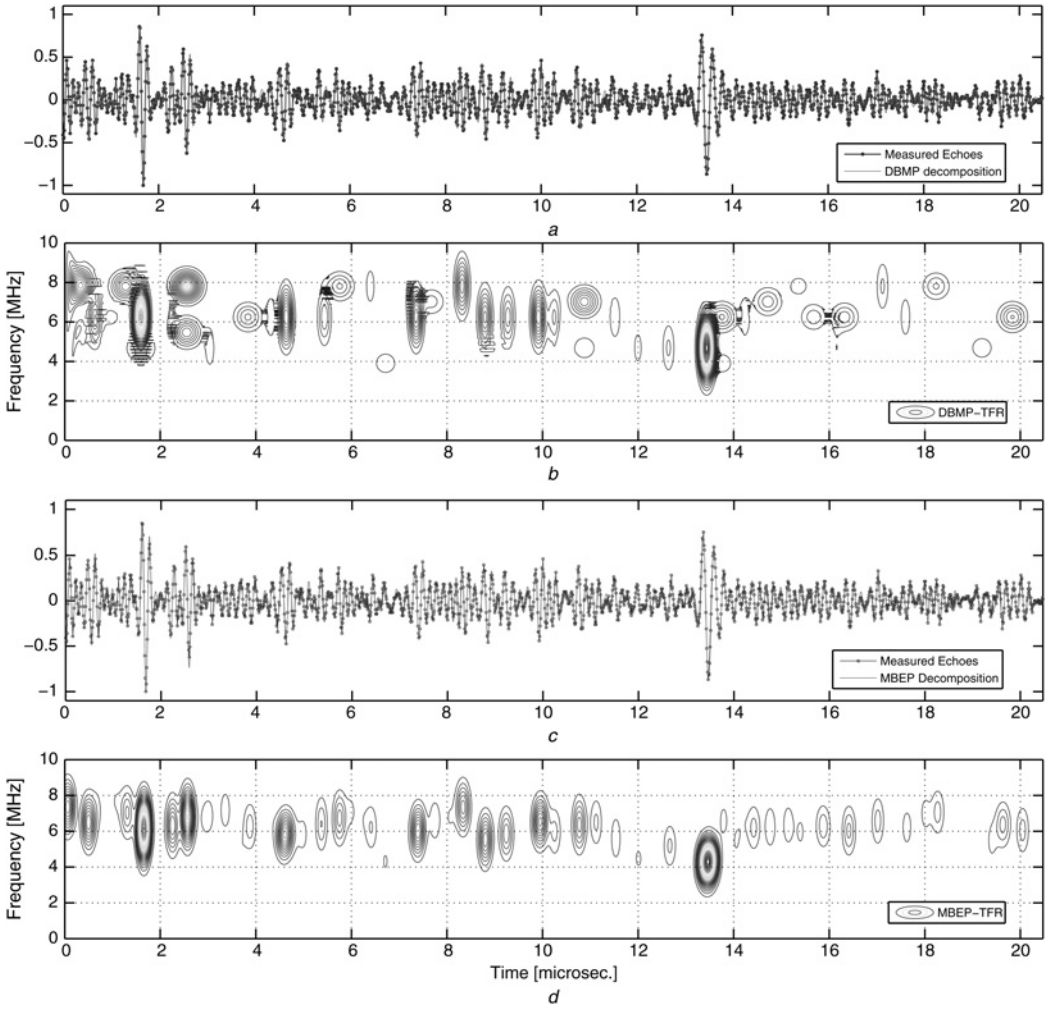


**Fig. 6** *Backscattered microstructure echoes with the flaw echo from the steel sample*

*a* Measured data (dotted line) and decomposition echoes (solid line) using DBMP
*b* TF contour plot of *a*
*c* Measured data (dotted line) and decomposition echoes (solid line) using MBEP
*d* TF contour plot of *c*

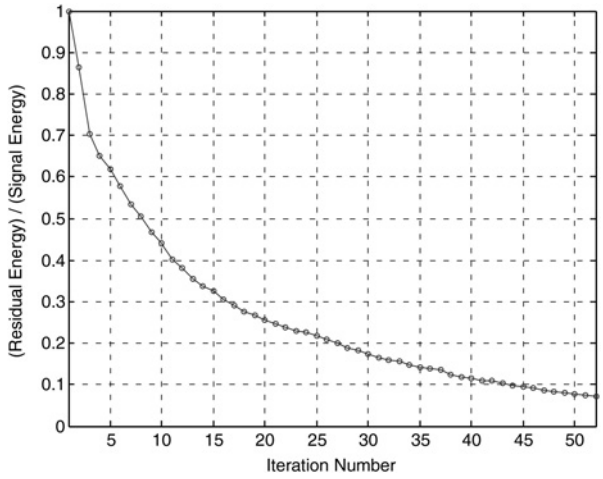


**Fig. 7** *Decline of normalised residual energy with MBEP iterations for real ultrasonic data presented in Fig. 6*

## 5 Conclusions

The conventional approach to sparse representation of ultrasonic echoes is the dictionary-based MP algorithm. The performance of this approach in extracting meaningful echo components is limited by the rigid structure of the pre-defined dictionary. Model-based signal decomposition methods utilising parametric models provide improved decompositions for echo analysis. However, they still use correlation in echo matching. In this study, we have developed MBEP algorithm based on statistical estimation techniques (MLE and MAP) to obtain sparse representation of ultrasonic signals in terms of model echoes that have certain desired characteristics. This algorithm offers several important advantages over the conventional DBMP and model-based decomposition algorithms. First, it provides a greater control and flexibility in extracting meaningful echo components by incorporating prior knowledge in signal decomposition. The prior knowledge can be obtained from the spectral characteristics of the measuring transducer. Second, it obtains a fine-tuned decomposition in terms of the kernel function via optimisation of model parameters. Finally, MBEP signal decomposition framework can utilise any specific echo models. As such, it can be used in the analysis of a variety of ultrasound signals such as scattering echoes from the microstructure of materials, reverberation echoes and dispersive waves. Following the guidelines in this paper one can develop a parameter estimation algorithm

using a specific model and incorporate prior knowledge in signal decomposition.

## 6 References


1 Mallat, S., Zhang, Z.: 'Matching pursuits with time-frequency dictionaries', *IEEE Trans. Signal Process.*, 1993, **41**, pp. 3397–3415
2 Lu, Y., Michaels, J.E.: 'Numerical implementation of the matching pursuit for the analysis of complex ultrasonic signals', *IEEE Trans. Ultrason. Ferroelectr. Freq. Control*, 2008, **55**, (1), pp. 173–182
3 Hong, J.C., Sun, K.H., Kim, Y.Y.: 'Waveguide damage detection by the Matching Pursuit approach employing the dispersion based Chirp functions', *IEEE Trans. Ultrason. Ferroelectr. Freq. Control*, 2006, **53**, (3), pp. 592–605
4 Cloutier, G.: 'A new clutter rejection algorithm for Doppler ultrasound', *IEEE Trans. Med. Imag.*, 2003, **22**, (4), pp. 530–538
5 Qian, S., Chen, D.: 'Signal approximation via data-adaptive normalized Gaussian functions and its applications for speech processing'. IEEE Int. Conf. on Acoustics, Speech, and Signal Processing, March 1992, vol. 1, pp. 141–144
6 Qian, S., Chen, D.: 'Signal representation using adaptive normalized Gaussian functions', *Signal Process.*, 1994, **36**, pp. 1–11
7 Demirli, R., Saniie, J.: 'A high-fidelity time-frequency representation for ultrasonic signal analysis'. Proc. IEEE Int. Ultrasonics Symp., October 2003, pp. 1376–1379
8 Demirli, R., Saniie, J.: 'Model-based estimation of ultrasonic echoes, part I: analysis and algorithms', *IEEE Trans. Ultrason. Ferroelectr. Freq. Control*, 2001, **48**, (3), pp. 787–802
9 Cardoso, G., Saniie, J.: 'Ultrasonic data compression via parameter estimation', *IEEE Trans. Ultrason. Ferroelectr. Freq. Control*, 2005, **52**, (2), pp. 313–325
10 Schwarzenberg, G.F., Weber, M., Hopp, T., Ruiter, N.V.: 'Model based pulse detection for 3D ultrasound computer tomography'. Proc. IEEE Int. Ultrasonics Symp., October 2007, pp. 1255–1258
11 Lu, Y., Demirli, R., Cardoso, G., Saniie, J.: 'A successive parameter estimation algorithm for chirplet signal decomposition', *IEEE Trans. Ultrason. Ferroelectr. Freq. Control*, 2006, **53**, (11), pp. 2121–2131
12 Lu, Y., Demirli, R., Saniie, J.: 'Efficiency and sensitivity analysis of chirplet signal decomposition for ultrasonic NDE applications'. Proc. IEEE Int. Ultrasonics Symp., October 2007, pp. 1590–1593
13 Kay, S.M.: 'Fundamentals of statistical signal processing: estimation theory' (Prentice Hall, NJ, 1993)
14 Demirli, R., Saniie, J.: 'An efficient sparse signal decomposition technique using envelope and instantaneous phase'. Proc. IEEE Int. Ultrasonics Symp., October 2008, pp. 1503–1507
15 Jaggi, S., Carl, W.C., Mallat, S., Willsky, A.S.: 'Feature extraction through high-resolution pursuit', *Appl. Comput. Harmon. Anal.*, 1998, **5**, (4), pp. 428–449
16 Gribonval, R., Bacry, E., Mallat, S., Depalle, Ph., Rodet, X.: 'Analysis of sound signals with high resolution matching pursuit'. Proc. IEEE Time-Frequency Time-Scale Analysis Symp., June 1996, pp. 125–128
17 Ferrando, S.E., Kolasa, L.A.: 'A flexible implementation of matching pursuit for Gabor functions on the interval', *ACM Trans. Math. Softw.*, 2002, **28**, (3), pp. 337–353


## 7 Appendix

### 7.1 MAP parameter estimation of GC function

We assume that the parameter vector $\boldsymbol{\theta}$ of GC function is a random variable with following statistics

$$E[\theta] = \bar{\theta} = \mu_\theta \quad \text{and} \quad E[(\theta - \bar{\theta})(\theta - \bar{\theta})^{\mathrm{T}}] = C_\theta \tag{15}$$

In order to obtain a best fit echo to a partitioned signal given in (6) ($R^n y_{\mathrm{p}} = g(\theta) + R^{n+1} y_{\mathrm{p}}$), we need to minimise the objective function $\gamma(\theta) = \|R^n y_{\mathrm{p}} - g(\theta)\|^2$ under the above prior statistics. However, the echo model $g(\theta)$ is a non-linear function of $\theta$, hence no closed-form solution is available. One can obtain an iterative estimator by successively linearising the model in the objective function. Hence, $g(\theta)$ is made linear using the Taylor series expansion at about a known parameter values $\theta^{(0)}$

$$g(\theta) \simeq g(\theta^{(0)}) + H(\theta^{(0)})(\theta - \theta^{(0)}) \quad \text{where}$$
$$H(\theta^{(0)}) = \left.\frac{\mathrm{d}g(\theta)}{\mathrm{d}\theta}\right|_{\theta=\theta^{(0)}}$$

where $H(\theta)$ is the gradients of the model. Using the approximation above, the observation model (6) can be made linear as

$$R^n y_{\mathrm{p}} = g(\theta^{(0)}) + H(\theta^{(0)})(\theta - \theta^{(0)}) + R^{n+1} y_{\mathrm{p}} \tag{16}$$

Rewriting the above equation as

$$\tilde{x} = H(\theta^{(0)})\theta + w \tag{17}$$

where $\tilde{x} = R^n y_{\mathrm{p}} - g(\theta^{(0)}) + H(\theta^{(0)})\theta^{(0)}$ and $w = R^{n+1} y_{\mathrm{p}}$. The above expression (17) is recognised as the Bayesian linear model, and the MAP estimator for this type of model is defined as [13]

$$\theta_{\mathrm{MAP}} = \mu_\theta + \left[C_\theta^{-1} + \frac{1}{\sigma_w^2} H^{\mathrm{T}}(\theta^{(0)}) H(\theta^{(0)})\right]^{-1} \times H^{\mathrm{T}}(\theta^{(0)}) \frac{1}{\sigma_w^2} [\tilde{x} - H(\theta^{(0)})\mu_\theta] \tag{18}$$

where $\mu_\theta$ and $C_\theta$ are the prior mean and covariance, respectively, and $\sigma_w^2$ is the noise variance for WGN model for $w = R^{n+1} y$.

$$\tilde{x}^{(k)} = R^n y_{\mathrm{p}} - g(\theta^{(k)}) + H(\theta^{(k)})\theta^{(k)}$$

$$\theta_{\mathrm{MAP}}^{(k+1)} = \mu_\theta + \left[C_\theta^{-1} + \frac{1}{\sigma_w^2} H^{\mathrm{T}}(\theta^{(k)}) H(\theta^{(k)})\right]^{-1} \times H^{\mathrm{T}}(\theta^{(k)}) \frac{1}{\sigma_w^2} [\tilde{x}^{(k)} - H(\theta^{(k)})\mu_\theta] \tag{19}$$

Using above iteration formulas, the MAP Gauss–Newton algorithm is formally outlined in the following steps:

*MAP Gauss–Newton (MAP–GN) algorithm*

1. Set prior statistics for the parameter vector

$$E[\theta] = \bar{\theta} = \mu_\theta \quad \text{and} \quad E[(\theta - \bar{\theta})(\theta - \bar{\theta})^{\mathrm{T}}] = C_\theta$$

2. Set the initial $\theta^{(0)}$as the prior mean and set $k = 0$ (iteration number).
3. Compute the gradients $H(\theta^{(k)})$and the GC function $g(\theta^{(k)})$.




doi: 10.1049/iet-spr.2011.0093

4. Iterate the parameter vector via MAP estimation

$$\tilde{x}^{(k)} = R^n y_{\mathrm{p}} - g(\theta^{(k)}) + H(\theta^{(k)})\theta^{(k)}$$

$$\theta_{\mathrm{MAP}}^{(k+1)} = \mu_\theta + \left[C_\theta^{-1} + \frac{1}{\sigma_w^2} H^{\mathrm{T}}(\theta^{(k)}) H(\theta^{(k)})\right]^{-1} \times H^{\mathrm{T}}(\theta^{(k)}) \frac{1}{\sigma_w^2} [\tilde{x}^{(k)} - H(\theta^{(k)})\mu_\theta]$$

5. Check convergence: If $\|\theta^{(k+1)} - \theta^{(k)}\| <$ tolerance, STOP.
6. Set $k \rightarrow k+1$ and go to Step 2.

$\boldsymbol{H}(\theta)$ in Step 4 denotes the gradient matrix, that is

$$\boldsymbol{H}(\theta) = \left[\frac{\partial g}{\partial \alpha} \quad \frac{\partial g}{\partial \tau} \quad \frac{\partial g}{\partial f_{\mathrm{c}}} \quad \frac{\partial g}{\partial \psi} \quad \frac{\partial g}{\partial \varphi} \quad \frac{\partial g}{\partial \beta}\right]$$

Each column represents the partial derivative of GC function with respect to a parameter. Analytical solutions are available for the gradient matrix $\boldsymbol{H}(\theta)$ [11]. Furthermore, the term $(H^{\mathrm{T}}(\theta)H(\theta))$ in Step 4 can be analytically computed to bypass inner product calculation. This will significantly accelerate the algorithm [8].

The above algorithm can be used as a MLE Gauss–Newton (MLE–GN) algorithm by assuming a very large covariance matrix, that is, by setting $C_{\theta\theta} \rightarrow \infty$ and by setting the prior mean as the initial guess, that is, $\mu_\theta = \theta^{(0)}$. In that case the iteration formula in Step 4 will reduce to

$$\theta_{\mathrm{MLE}}^{(k+1)} = \theta^{(k)} + ((H^{\mathrm{T}}(\theta^{(k)})H(\theta^{(k)}))^{-1} H^{\mathrm{T}}(\theta^{(k)})(R^n y - g(\theta^{(k)})) \tag{20}$$

which is essentially the GN iteration formula without priors. Using above formula in Step 4, the MAP–GN algorithm will become a MLE–GN algorithm which has been presented in [8] for a Gaussian echo model.